Synthesis and Characterization of Long Perylenediimide Polymer Fibers: From Bulk to the Single-Molecule Level

Pieter A. J. De Witte,[†] Jordi Hernando,*[,‡,§] Edda E. Neuteboom,[||] Erik M. H. P. van Dijk,[‡] Stefan C. J. Meskers,[||] René A. J. Janssen,[||] Niek F. van Hulst,[‡,⊥,¶] Roeland J. M. Nolte,*[,†] Maria F. García-Parajó,[‡,¶,#] and Alan E. Rowan*[,†]

Institute for Molecules and Materials, Toernooiveld 1, 6525 ED, Nijmegen, The Netherlands, Applied Optics, University of Twente and MESA+ Institute for Nanotechnology, P.O. Box 217, 7500 AE Enschede, The Netherlands, Departament de Química, Universitat Autònoma de Barcelona, 08193 Cerdanyola del Vallès, Spain, Laboratory of Macromolecular and Organic Chemistry, Eindhoven University of Technology, P. O. Box 513, 5600 MB Eindhoven, The Netherlands, ICFO (Institut de Ciències Fotòniques), 08860 Castelldefels, Spain, ICREA (Institució Catalana de Recerca i Estudis Avançats), 08010 Barcelona, Spain, and Laboratory of NanoBioengineering, Parc Científic de Barcelona (PCB), Josep Samitier 1−5, 08028 Barcelona, Spain

Received: December 2, 2005; In Final Form: February 20, 2006

The synthesis and characterization of perylenediimide polyisocyanides is reported. In addition to short oligomers, our synthetic approach results in the formation of extremely long, well-defined, and rigid perylenediimide polymers. Ordering and close-packing of the chromophores in these long polymers is guaranteed by attachment to a polyisocyanide backbone with amino acid side chains. Hydrogen bonding interactions between those groups stabilize and rigidify the helical polymer structure. The rodlike nature of the synthesized long perylenediimide pendant polyisocyanides as well as the helical arrangement of the chromophores is demonstrated by means of atomic force microscopy. Remarkably, polymer fibers up to 1 μm in length have been visualized, containing several thousands of perylenediimide molecules. Circular dichroism spectroscopy reveals the chiral organization of the chromophore units in the polymer, whereas absorption and emission measurements prove the occurrence of excited-state interactions between those moieties due to the close packing of the chromophore groups. However, an intricate optical behavior is encountered in bulk as a result of the coexistence of short oligomers and long polymers of perylenediimide, a situation subsequently uncovered by means of single-molecule experiments. Individual long helical perylenediimide polyisocyanides exhibit a typical red-shifted fluorescence spectrum, which, together with depolarized emission continuously decreasing in time, demonstrate that fluorescence arises from multiple excimer-like species in the polymer. Upon continuous irradiation of these long polymers, a fast decay in fluorescence lifetime is observed, a situation explained by photoinduced creation of quenching sites. Radical/ion formation by intramolecular electron transfer between close-by perylenediimide moieties is the most probable mechanism for this process. Appropriate control of the electron-transfer process might open the possibility of applying these polymers as perylenediimide-based supramolecular nanowires.

Introduction

Whereas most organic conducting species behave as p-type semiconductors, materials based on perylenediimide (PDI) derivatives are known to support electron transport through the conduction band.[1] This feature, together with a strong absorptivity in the visible region of the spectrum and a high thermal and photochemical stability, makes perylenediimide compounds promising candidates as n-type semiconductors in organic photovoltaic cells. Indeed, several types of organic solar cells in which PDI is used as n-type material have recently been reported.[2] However, so far these devices exhibit a rather low energy conversion efficiency (η) compared to conventional inorganic cells. Improvement of η requires an increase in the exciton-diffusion length upon light absorption as well as in the transport of charge carriers after exciton dissociation. A well-ordered arrangement of the organic moieties in the conducting material has been shown to favor the accomplishment of these conditions.[2c,3] In fact, it has been demonstrated that increased ordering of the PDI molecules leads to higher exciton-diffusion lengths,[4] stabilizes charge-separated states,[5] and enhances electron mobilities.[2c] As such, the construction of well-defined perylenediimide assemblies is an important area of research with potentially interesting applications.

Close-packing and ordering of PDI molecules at the nano- and microscale are usually attained by self-organization,[6] a process driven by $\pi-\pi$ stacking,[2b,c,7] hydrogen bonding,[8] metal−ligand interactions,[9] or electrostatic forces.[10] However, only a limited control over the final structures can be achieved in this way. An attractive alternative is to construct perylenediimide assemblies by means of covalent synthesis. Unfortu-

* To whom correspondence should be addressed. E-mail: jordi.hernando@uab.es (J.H.); r.nolte@science.ru.nl (R.J.M.N.); a.rowan@science.ru.nl (A.E.R.).
† Institute for Molecules and Materials.
‡ University of Twente and MESA Insitute for Nanotechnology.
§ Universitat Autònoma de Barcelona.
|| Eindhoven University of Technology.
⊥ ICFO.
¶ ICREA.
# PCB.

10.1021/jp057009d CCC: $30.25
Published on Web 03/25/2006

SCHEME 1: Synthesis of PDI Pendant Polyisocyanide 8[a]

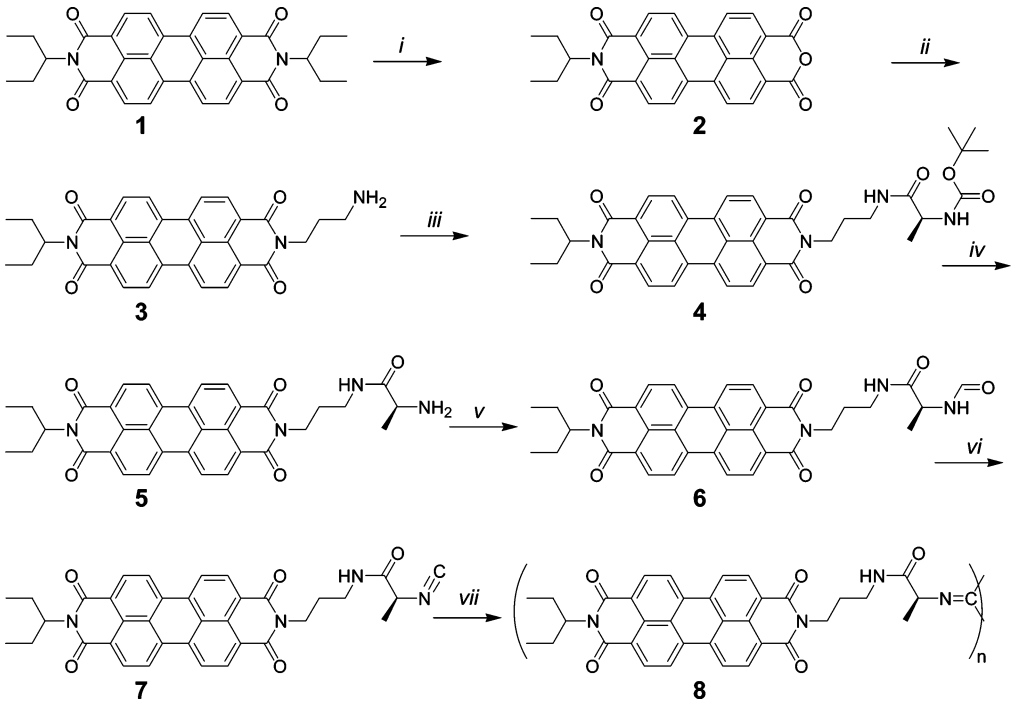

[a] (i) KOH, *tert*-buthanol; (ii) 1,3-diaminopropane, DMF, 100 °C, 2 h; (iii) *Boc*-L-ala, DCC/DMAP, CH_2Cl_2, 0 °C; (iv) TFA, CH_2Cl_2; (v) formyl-ONP, CH_2Cl_2; (vi) diphosgene/NMM, CH_2Cl_2, 0 °C; (vii) $Ni(ClO_4)_2$/ethanol, $CHCl_3$.

nately, it is difficult to conciliate the requirements of a well-defined and close-packed arrangement of the molecules with a facile covalent synthesis of large structures. Indeed, mainly dendrimers[11] and low molecular weight polymers[12] containing perylenediimide or, alternatively, perylenemonoimide moieties have been reported so far. To tackle this problem, we have recently proposed to prepare long and well-ordered arrays of chromophores by covalently attaching them to a rigid polyisocyanide backbone. Our approach relies on the use of amino acid derived isocyanide precursors, which promote the occurrence of hydrogen bonding interactions between the side chains of the resulting polymer. These hydrogen bonds rigidify and stabilize the polyisocyanide helical structure.[13] So far we have exploited this approach to the synthesis of well-defined porphyrin anchored polymers, which were found to be stiff rods with an average length of 87 nm.[14] Photophysical studies showed that the stacks of porphyrins along the polymer chain display exciton migration and that the exciton diffusion length extends over at least 10 nm.[14]

In this paper we report on a similar strategy to prepare perylenediimide pendant polyisocyanides. Very long arrays (up to 1 μm in length) of well-organized and close-packed PDI moieties have been synthesized by means of covalent coupling. We have used atomic force microscopy (AFM) to investigate the shape and dimensions of the individual polymer molecules. Furthermore, the optical properties of the new perylenediimide-based structures have been studied in detail. Bulk measurements reveal exciton interactions between nearby chromophores in the perylenediimide polyisocyanides, as well as an intricate dependence of their photophysical properties on the polymer length. In a recent communication, we have shown that the combination of AFM and single-molecule spectroscopy (SMS) can be used to address the latter issue.[15] Here we further exploit the ability of SMS to report on the properties of heterogeneous populations of molecules to specifically investigate the optical behavior of the technologically relevant, long perylenediimide anchored polymers.

Results and Discussion

Synthesis. For the synthesis of PDI pendant polyisocyanide **8**, the perylenediimide **1** was used as the starting material (Scheme 1).[16] This compound was partially hydrolyzed with potassium hydroxide in *tert*-buthanol to give the anhydride imide **2**,[17] which was subsequently reacted with 1,3-diaminopropane in dimethylformamide (DMF) to afford the asymmetric perylenediimide **3**. The latter compound was coupled to *tert*-butyloxycarbonyl-L-alanine (*Boc*-L-ala)) using dicyclohexylcarbodiimide (DCC) and *N*,*N*-(dimethylamino)pyridine (DMAP) as a catalyst. The *Boc*-protecting group was cleaved off with trifluoro acetic acid (TFA), and the resulting amine **5** was reacted with *p*-nitrophenylformate (formyl-ONP) to give formamide **6**, which was dehydrated with diphosgene and *N*-methylmorpholine (NMM) as base to yield the isocyanide **7**. Polymerization of **7** was carried out using Ni(II) as a catalyst (0.002 equiv), resulting in polymer **8**. The resulting polymer was moderately soluble in organic solvents such as chloroform and toluene, thus facilitating the subsequent processing.

The infrared spectra of all precursors **1**−**7** clearly showed the presence of characteristic C−H out of plane wagging absorptions around 810 and 750 cm^{-1}, O═CN stretching vibrations around 1700 and 1660 cm^{-1} and C═C aromatic stretching vibrations around 1590 and 1575 cm^{-1}, as previously reported for other perylenediimide derivatives.[18] The infrared spectrum of isocyanide monomer **7** additionally displayed N≡C stretching vibration at 2142 cm^{-1} and an N−H stretching vibration at 3355 cm^{-1}. In contrast, the IR spectrum of polymer **8** showed complete disappearance of the isocyanide group stretching vibration as well as a significant shift of the N−H stretching vibration toward 3286 cm^{-1}. Together with smaller changes in the 1550−1700 cm^{-1} region, these features indicate not only the formation of a polyisocyanide backbone but also the presence of hydrogen bonding interactions between the amide groups of the polymer side chains.[19] According to

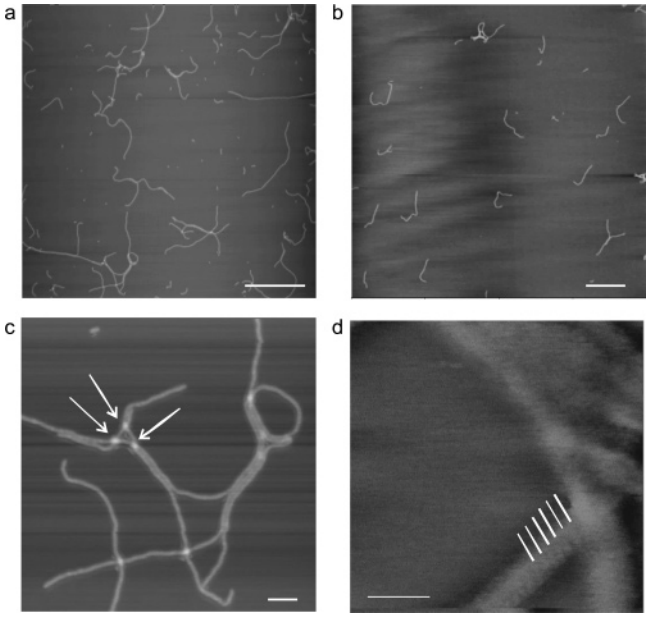

Figure 1. (a, b) AFM images of spin-coated $CHCl_3$ solutions of polymer **8** on mica (bar = 500 nm): (a) concentrated polymer solution; (b) diluted polymer solution. (c, d) Magnification of areas of a ((c) bar = 50 nm; (d) bar = 10 nm). The arrows in c indicate crossing points between different fibers. The parallel solid lines in d highlight the helical pitch observed for individual fibers.

previous studies by our group,[13,14,19] such interactions lead to stabilization of the 4_1 helical structure of polyisocyanides. A stable rodlike structure is therefore also expected for compound **8**.

Atomic Force Microscopy. Due to its rodlike nature, high molecular weight (see below) and moderate solubility, polymer **8** could not be characterized by neither MALDI-TOF MS nor GPC. Instead, AFM was used to investigate the shapes and dimensions of the PDI pendant polyisocyanides. Spin-coated $CHCl_3$ solutions of **8** revealed the presence of isolated fiberlike structures regardless of the polymer concentration (Figure 1a,b). All fibers in the AFM images displayed uniform height (2.5 nm) and diameter (5.5 nm), which were preserved over their entire length. Accordingly, we assign the fiberlike features to single PDI pendant polyisocyanides. Indeed, the polymer width calculated for an isolated chain of polyisocyanide **8** by means of molecular modeling (5.0)[20] satisfactorily agrees with the experimental observation. The measured height, however, is only half the calculated diameter, which is an artifact most probably arising from tip−sample interactions.[21]

Despite their equal height and width, the isolated PDI polyisocyanides in the AFM images exhibited a rather broad length distribution, as illustrated by the polymer contour length distribution shown in Figure 2. Clearly, the features in the AFM images range from a few nanometers up to more than a micrometer in length. Applying the formulas in ref 14 to the distribution in Figure 2, a number average length of 178 nm and a length polydispersity of 2.3 are determined for the synthesized PDI polyisocyanides. From molecular modeling calculations, we know that every isocyanide monomer must add ∼0.1 nm to the polymer backbone of compound **8**.[13a] Therefore, PDI polymers must contain, on average, more than a thousand chromophore units (degree of polymerization ∼ 1780), rendering a number average molecular mass as high as ca. 1.0×10^7 Da. To the best of our knowledge, such large perylenediimide-based arrays prepared by covalent coupling have not been described before.

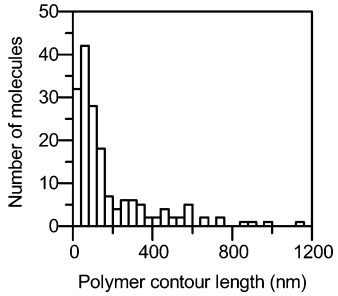

Figure 2. Distribution of polymer contour lengths derived from the contours measured for 173 isolated perylenediimide polyisocyanides in several AFM images.

Interestingly, the AFM images suggest that single PDI polyisocyanides have a tendency to align at high concentrations, which is a common feature of rodlike objects. Such a behavior is clearly visible in Figure 1c, where a particular area of Figure 1a is enlarged. Crossing points between single fibers are visible as higher topographical features in the image, while the assembly of two or more fibers results in an evident increase of the width of the imaged structures.

At even higher magnification a blurry fine structure is distinguishable on the single polymer fibers, which is suggestive of the occurrence of a helical architecture (Figure 1d). The presence of a regular substructure in the fiber is more clearly seen in Figure 3a, where a height cross-section along the polymer axis is depicted. To our knowledge, this is the first observation of a helical structure in a single synthetic polymer fiber by means of AFM. Measured on several samples, the helices were found to have a pitch of ca. 1.5 nm. Although it is tempting to relate the observed helicity to the helical backbone of the polyisocyanide polymers, the explanation of the measured pitch is not straightforward. Since every perylenediimide isocyanide monomer adds ∼0.1 nm to the backbone of polymer **8**, a pitch of 1.5 nm is tentatively interpreted as involving 15 PDI units, i.e. chromophore number 16 must be on top of chromophore 1. This would result in a projection angle between perylenediimide 1 and 5 (β) of 24° (Figure 3b). According to this angle and a distance of 1.7 nm from the middle of the polymer backbone to the center-of-mass of the chromophores obtained by molecular modeling, the center-of-mass intermolecular separation between PDI units 1 and 5 must then be ca. 0.8 nm. Figure 3c displays a schematic 3D drawing of the perylenediimide polyisocyanide structure which is consistent with such geometrical parameters.

Absorption and Circular Dichroism Spectroscopy. Figure 4a shows the absorption spectra of monomer **7** and polymer **8** in $CHCl_3$. The monomer **7** spectrum displays several well-defined peaks in the 400−550 nm region, whose maxima are located at λ_{max} = 432, 459, 490, and 527 nm. These peaks correspond to different vibronic bands (3−0, 2−0, 1−0, and 0−0, respectively) associated with the PDI main transition dipole moment, which is aligned along the long axis of the molecule. Although polymer **8** also shows several absorption bands in the 400−550 nm region, their maxima (λ_{max} = 469, 492, and 533 nm), relative intensity, and width are different from those of the monomer.

The changes in the absorption spectra are indicative of the presence of strong Coulombic (exciton) interactions between the transition dipole moments of nearby PDI moieties in polymer **8**.[7,22] Compared to the sharp vibronic peak at 527 nm of monomer **7**, a low-intensity band appears for polymer **8** at longer wavelengths and the absorption at ∼490 nm increases. Such a blue shift of the absorption maximum and an accompanying

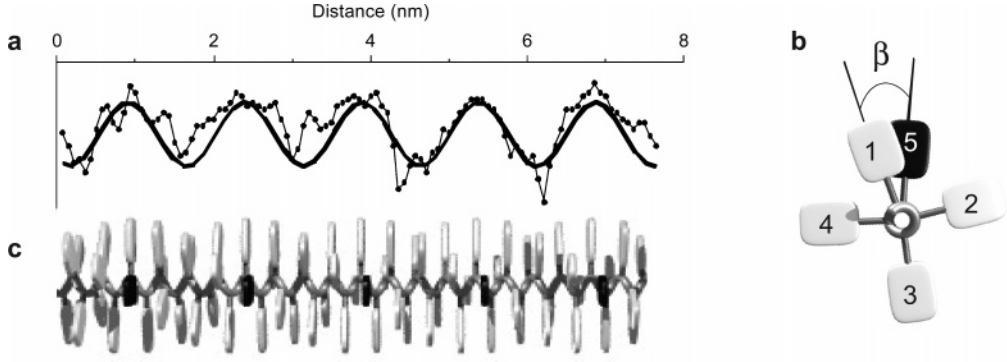

Figure 3. (a) Height cross-section along the axis of a single perylenediimide polyisocyanide imaged by means of AFM (see Figure 1d). The measured profile is depicted as connected dots, while the solid thicker line shows a tentative fitting using a cosine function. A pitch of ≈1.5 nm is clearly visible. (b) Schematic top view of a polymer **8** molecule consisting of five PDI units attached to a helical polyisocyanide backbone. The projection angle between perylenediimides 1 and 5 is $\beta = 24°$, as measured by AFM. (c) Schematic side view of polymer **8** with $\beta = 24°$. The black disks are the PDI units i, $i + 16$, $i + 32$, $i + 48$, ..., which fall one on top of each other leading to the pitch of 1.5 nm observed in the AFM images. For the sake of simplicity, a perpendicular orientation of the PDI moieties with respect to the polymer backbone is assumed in the drawing.

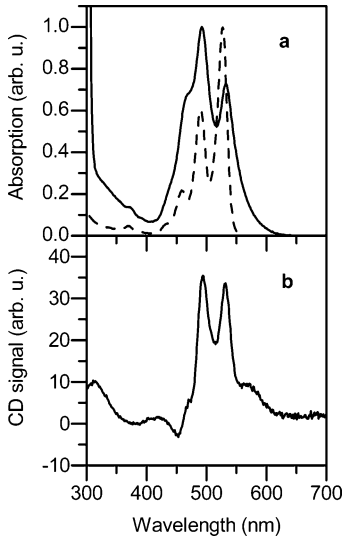

Figure 4. (a) Absorption spectra of monomer **7** (dashed line) and polymer **8** (solid line) in chloroform. (b) Circular dichroism (CD) of polymer **8** in chloroform. Similar results are obtained with toluene as solvent. The CD spectrum of **7** is not plotted, as it does not show any feature.

low-intensity band at lower energy has previously been reported for perylenediimide assemblies in which the transition dipole moments of adjacent chromophores are parallel or make a small angle.[7c,e,22] According to the chromophore orientation inferred from AFM (Figure 3), a similar situation is expected for polymer **8** if we take into consideration that the interaction of the transition dipole moments of perylenediimides i and $i + 4$ ($\beta = 24°$) will be much larger than the interactions in other pairs because of the shorter interchromophoric distance (∼0.8 nm), thus dominating the pattern of the excitonic levels.[23] Applying exciton theory to the dipole−dipole coupling for such a dimeric unit,[24] a blue shift of ca. 19 nm and a red shift of ca. 20 nm are predicted for the aggregate compared to the monomer absorption band. The deviation from the experimental observations for the aggregate spectrum in Figure 4a (e.g. blue shift ∼ 37 nm) suggests that a more complex model accounting for the interaction in all chromophore pairs and their helical arrangement is required. Indeed, for such a dye configuration, exciton theory[25] also predicts the splitting of the monomer absorption spectrum in a blue- and a red-shifted bands, as previously observed for porphyrin polyisocyanides.[14] The considerable line width, however, prohibits further analysis of this fine structure. In addition, the overlap of the excitonic bands with the perylenediimide vibronic structure further complicates the appearance of the spectrum and makes it difficult to quantitatively interpret the bulk polymer absorption spectrum in Figure 4a. Nevertheless, since strong exciton effects only hold for short interchomophoric distances, the measured absorption spectra confirm the close-packing of PDI molecules in polymer **8**.

Figure 4b shows the circular dichroism (CD) spectrum of the perylenediimide polyisocyanide in $CHCl_3$. While monomer **7** displays no detectable CD effect (not shown), several interesting features are observed for the PDI pendant polyisocyanide. A positive Cotton signal appears within the 300−350 nm region, which is ascribed to the imine groups present in the polymer **8** backbone. Such an effect is expected for helical polyisocyanides,[26] thus substantiating that the incorporation of the PDI moieties in the polymer keeps its backbone intact. Determination of the helix sense of the polymer from this CD signal is, however, hampered by side-chain contributions to the Cotton effects in this spectral region.[26]

Strong positive Cotton signals are observed for polymer **8** in the 450−550 nm region where the absorption bands due to interacting perylenediimides arise. These CD signals provide further support for the helical conformation of the synthesized polyisocyanide. It should be noted that a bisignated Cotton effect instead of a single positive band is predicted for such a type of chromophoric arrangement, and this prevents any precise conclusion about the helicity of the polymer. It is possible that the CD effects in polymer **8** are a combination of the helical orientation of perylenediimides and a helical twisting of the planar PDI into an axially chiral chromophore.[7d,8b]

The temperature-dependent behavior of the CD spectrum of polymer **8** was studied in $CHCl_3$ (up to 65 °C) and in toluene (up to 90 °C). No significant spectroscopic changes were observed in these two solvents upon heating (data not shown), indicating that the helical PDI architecture of polymer **8** is extremely stable. Only at very high temperatures (in toluene at 90 °C), a slight decrease of the CD signals was observed (ca. 25%), which nearly returned to their original values upon cooling. Such a decrease may result from the breaking of some hydrogen bonds in the polymer chain as well as from an increase in the random thermal motion of the PDI molecules.

Fluorescence Spectroscopy. The fluorescence emission spectra of monomer **7** and polymer **8** are shown in Figure 5a. As expected for PDI monomers, a strong and a weaker vibronic band is observed for monomer **7**, whose maxima are located at $\lambda_{max} = 535$ and 578 nm, respectively. Interestingly, the emission

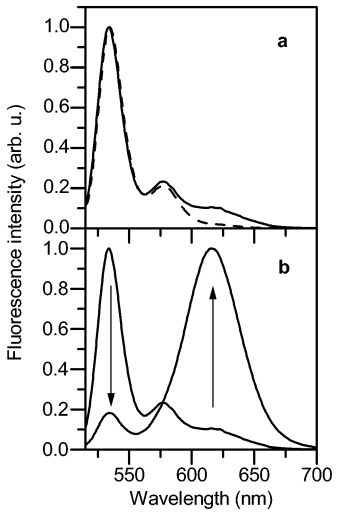

Figure 5. (a) Fluorescence emission spectra of monomer **7** (dashed line) and polymer **8** (solid line) in $CHCl_3$ ($\lambda_{exc} = 492$ nm). (b) Change of the fluorescence emission spectrum of compound **8** upon increasing the molecular weight of the polymer molecules by means of a fractionation experiment.

spectrum of polymer **8** also displayed the same peaks, together with an additional broad band at 620 nm. The occurrence of such red-shifted fluorescence band is consistent with the formation of perylenediimide excimer-like species in polymer **8**, a well-known phenomenon occurring in close-packed stacks of PDI molecules which is favored by exciton interactions and charge transfer.[7c,22,27] Since the polymer absorption spectrum differs from that of the monomer, we cannot exclude that interactions in the ground state also contribute to the formation of excimer-like species.[28]

In general, the formation of excimer-like species in solutions of chromophores is a concentration-dependent intermolecular process, whose fingerprint in the emission spectrum is a structureless red-shifted fluorescence band that decreases upon dilution. Concentration-dependent fluorescence studies on polymer **8**, however, revealed that the relative intensity of the excimer-like band compared to the monomer bands did not change. This result clearly indicates that excimer-like species formation in **8** is intramolecular in nature; i.e., it occurs within a single polymer chain.

To investigate the origin of the monomer-like and excimer-like bands in the bulk perylenediimide polyisocyanide emission spectrum, a fractionation experiment was carried out in which the polymer molecules were separated by size. Starting from the initial reaction mixture, fractionation was achieved by successive dissolution and precipitation cycles of a polymer **8** sample. The emission spectra of the higher molecular weight fractions obtained in this way displayed a very strong excimer-like emission, whereas the fractions containing the low molecular weight compounds mainly yielded monomer-like fluorescence (Figure 5b). Analogously, the corresponding absorption spectra were also significantly different (Figure S1 in the Supporting Information), either resembling the spectrum of polymer **8** (high molecular weight fractions) or that of monomer **7** (low molecular weight fractions). The measured fluorescence quantum yield of the higher molecular weight fractions relative to PDI monomer was 0.11. Such a decrease is to be expected for excimer-like emission in perylenediimide assemblies.[7c]

The fractionation experiment suggests that different polymer architectures within the same sample give rise to different optical properties. Fractions containing the lower molecular weight compounds with monomer-like absorption and fluorescence must correspond to short perylenediimide polyisocyanide oligomers and nonreacted isocyanide monomers left in the reaction mixture. For such short oligomers, no helical structure and hence a less well organized stack of PDI molecules are expected,[29] leading to weak or no exciton interactions between nearby chromophores and thus a monomer-like absorption and fluorescence spectra. Moreover, the absence of a defined helical structure prevents these species from being detected by means of atomic force microscopy, since their height falls below the sensitivity of our AFM instrument. On the other hand, the fractions containing the higher molecular weight compounds with strong exciton effects in the absorption and excimer-like emission must correspond to long PDI pendant polyisocyanides with a helical backbone, which can therefore be visualized in the AFM images due to their significant height. As mentioned above, the close-packed arrangement of the PDI molecules in such high molecular weight species must lead to strong exciton interactions between nearby chromophores as well as must be responsible for the formation of excimer-like species. Due to their lower energy, such excimer-like species trap the delocalized excitons created upon excitation, thus preventing direct emission from the exciton states. Instead, red-shifted fluorescence arising from the excimer-like sites is eventually detected. In a combined AFM and single molecule fluorescence spectroscopy investigation of polymer **8**, we unambiguously demonstrated the validity of such interpretation of the intricate optical behavior of PDI pendant polyisocyanides.[15] We also showed that most of the molecules displaying monomer-like emission in polymer **8** samples could be assigned to short polyisocyanide oligomers decorated with few PDI moieties.

We also recorded the fluorescence decay for the singlet excited state of monomer **7** and polymer **8** in $CHCl_3$. While the monomer decay is monoexponential with a characteristic lifetime value (τ) of 3.9 ns, as expected for nonsubstituted perylenediimides,[27] the fluorescence decay of polymer **8** could be fitted to a double-exponential function, resulting in lifetime values of $\tau = 3.9$ and 19.9 ns. The first of these values matches the result obtained for the PDI monomer precursor, whereas the second, much longer lifetime is typical for excimer-like species.[7c,22,27] This observation provides further evidence for the existence of two different species in polymer **8** samples. Indeed, in agreement with the reasoning given above, the contribution of the low, monomer-like τ value to the total fluorescence decay was found to significantly decrease when going from the initial polymer mixture to the higher molecular weight fractions of the PDI pendant polyisocyanides, thus indicating the predominance of excimer-like emission for the long helical polymers.

Single-Molecule Fluorescence Spectroscopy. As already discussed, bulk measurements of the optical properties of PDI pendant polyisocyanides suffer from the occurrence of different polymer architectures in the samples and the large spread in polymer lengths. On the other hand, SMS allows the behavior of individual emitting species to be probed, thus overcoming the problem of the heterogeneous behavior of the polymer **8** samples. We applied SMS to thoroughly investigate the optical properties of long helical perylenediimide polyisocyanides. To that end, we focused on the higher molecular weight fractions of compound **8** derived from the fractionation experiment. For the sake of comparison, the fluorescence behavior of individual monomer PDI molecules was also studied.

Figure 6 shows $10 \times 10\ \mu m^2$ fluorescence images of (a) PDI monomer and (b) PDI polymer molecules embedded in a thin layer of poly(methyl methacrylate) (PMMA). Isolated spots

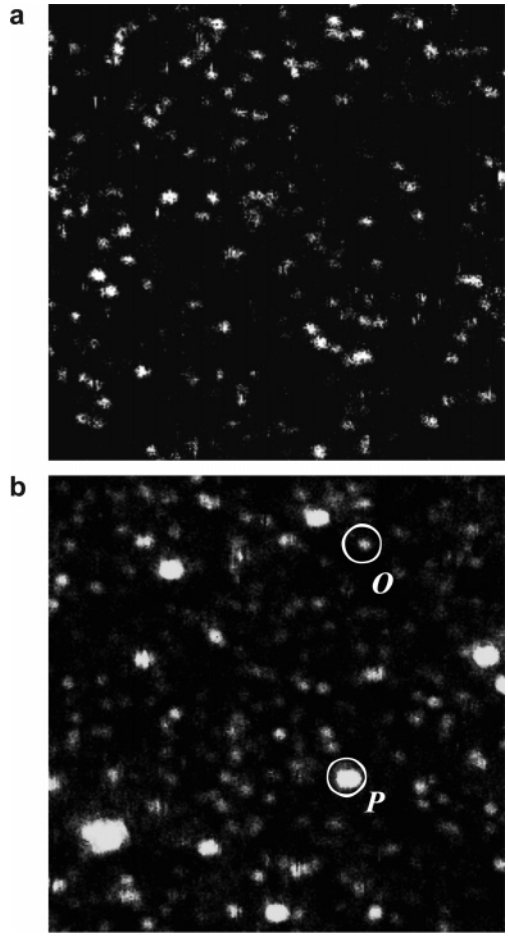

Figure 6. Fluorescence confocal images of $10 \times 10\ \mu m^2$ areas of (a) PDI monomer/PMMA and (b) PDI polyisocyanide/PMMA samples. *O* and *P* stand for diffraction-limited and larger fluorescence spots, respectively.

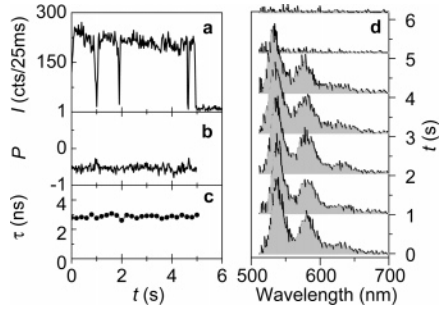

Figure 7. (a−d) Fluorescence intensity (I), polarization anisotropy (P), lifetime (τ), and spectrum trajectories of an individual PDI monomer. P is defined as $P = (I_x - gI_y)/(I_x + gI_y)$, where I_x and I_y are the emission components detected in two orthogonal polarization directions and g is an experimental factor accounting for their different detection efficiencies. P quantifies the degree of the polarization of fluorescence emission, taking the limiting values $+1/-1$ for linear polarized light in one of the two orthogonal polarization directions detected and being equal to 0 for fully depolarized emission. Each τ value is derived from a monoexponential fitting to the photon arrival time decay built every 200 ms.

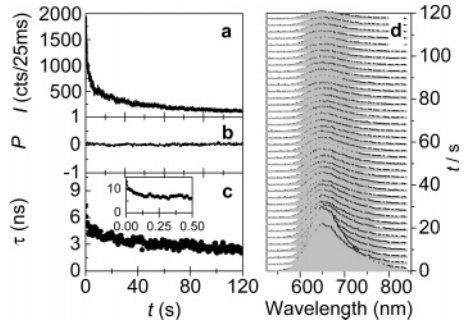

Figure 8. (a−d) Fluorescence intensity (I), polarization anisotropy (P), lifetime (τ), and spectrum trajectories of a single perylenediimide polyisocyanide molecule (type *P*). Each τ value does not derive from a fitting to the photon arrival time decay, but corresponds to the average photon arrival time determined every 400 ms (see Figure S2 in the Supporting Information). The inset in c shows the characteristic lifetime values obtained in this way every 20 ms for the first 0.5 s of the trace.

corresponding to individual emitting entities are observed in these images. While only diffraction-limited features (fwhm $\approx$ 235 nm) arising from the finite optical resolution of the microscope are found in the monomer image, both diffraction-limited and much larger spots are detected in the polymer sample, as illustrated by spots *O* (fwhm = 245 nm) and *P* (fwhm = 395 nm) in the figure. The occurrence of large fluorescence features was observed even for further diluted samples, indicating that they do not correspond to clusters of small, diffraction-limited spots but are due to long individual fibers (ca. length > 100 nm). The presence of such long polymers was already unambiguously demonstrated by the AFM images in Figure 1.[30]

The fluorescence properties of the individual small and large spots in perylenediimide polyisocyanides samples as well as those of the monomer molecules were further investigated by simultaneously detecting in time their fluorescence intensity, polarization, lifetime, and spectrum. Figure 7 shows as an example the typical behavior found for individual PDI monomers. As previously observed by others for similar chromophores[31] and illustrated by Figure 7a, most of the single PDI molecules analyzed (55 out of 67) displayed a rather stable fluorescence signal in time, a monotonic behavior only interrupted by reversible trap formation (t = 1, 2, and 4.7 s in Figure 7a), such as triplet states or radical ions[31,32] and eventually by an irreversible photobleaching (t = 5 s in Figure 7a). Analogously, these molecules did not show significant time variations in the fluorescence lifetime and spectrum (Figure 7c,d), reproducing the PDI monomer behavior in bulk. The few molecules showing multiple signal levels in fluorescence (18%) presented spectral jumps or spectral and lifetime changes correlated with intensity fluctuations, processes typically ascribed to changes in the molecule nanoenvironment and photoinduced reactions, respectively.[33,34] The fluorescence polarization anisotropy (Figure 7b) was constant and different from zero, consistent with a single dipole emission.

The fluorescent species in the PDI polymer samples displayed two different optical behaviors (types *P* and *O*). This situation is summarized in Figures 8 and 9. Clearly, both types of species differ with respect to their intensity, polarization, lifetime, and spectral properties. Type *P* behavior is observed for all the large isolated features in the fluorescence images of the PDI polymer samples, as well as for some of the small, diffraction-limited spots. The remaining of those small features exhibit type *O* behavior. In total, ca. 20% of the fluorescent species analyzed in the PDI polymer samples corresponded to type *P* and ca. 80% to type *O*.

Figure 8a shows the fast and monotonic decay of the fluorescence signal typically arising from a type *P* molecule upon continuous irradiation. The shape of its structureless, broad, and red-shifted fluorescence spectrum remains constant in time (Figure 8d). These features are consistent with multiple excimer-like emitting sites in the molecule, which become sequentially bleached. In that case, stepwise changes of the fluorescence intensity are expected at the end of the trace, when very few or

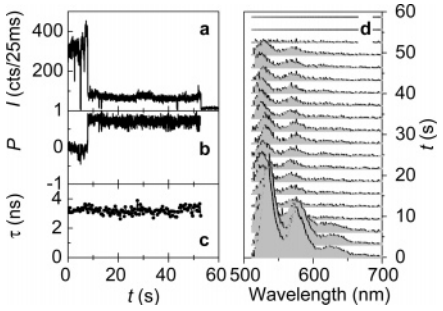

Figure 9. (a−d) Fluorescence intensity (*I*), polarization anisotropy (*P*), lifetime (τ), and spectrum trajectories of a single perylenediimide polyisocyanide (type *O*). Each τ value is derived from a monoexponential fitting to the photon arrival time decay built every 400 ms.

even a single emitting site remains active. However, this behavior was hardly observed in type *P* molecules due to the low fluorescence quantum yield of excimer-like species in the polymers (see below), which made it difficult to detect the emission arising from only a few of these sites. On the other hand, a discrete number of defined intensity levels occurred in the time trajectories of type *O* species (Figure 9a). Thus, 36, 45, and 19% of these molecules show one, two, and three or more intensity levels in their fluorescence, respectively. In all cases, both their fluorescence lifetime (Figure 9c) and spectra (Figure 9d) resemble those of the monomer and they show no contribution from excimer-like species emission. This indicates that only one or a few emitting sites exist in type *O* molecules, which are weakly or not excitonically coupled and successively photobleached in a stepwise manner. Because larger spots are visible for type *P* molecules in the fluorescence images, the difference in the amount of emitters for both types of PDI polyisocyanides must be related to their sizes. Moreover, their distinct spectral features suggest different degrees of chromophore packing. These observations, which are also supported by the bulk fractionation experiment reported above, are definitely in line with our previously published combined AFM and SMS study of individual perylenediimide pendant polyisocyanides on glass.[15] It allows us to conclude that (i) type *P* behavior arises from long PDI polymers exhibiting the typical helical structure of polyisocyanides, whose length varies from tens to hundreds of nanometers, and (ii) type *O* behavior stems from much shorter nonhelical PDI oligomers together with some remaining nonreacted PDI monomers. Because large excitonically coupled arrays of PDI moieties are technologically more relevant, we will focus in the following on the description of type *P* species at the single-molecule level.

Figure 8b depicts the fluorescence polarization anisotropy trajectory of a long helical PDI polyisocyanide molecule. Upon continuous photobleaching of the excimer-like emitting sites in the polymer, no changes in *P* are observed. This parameter takes a constant value around zero regardless of the fluorescence intensity and indicates depolarized emission from the molecule. All type *P* polyisocyanides investigated displayed the same behavior. In contrast, the individual PDI monomers had well-defined values of the polarization anisotropy parameter that were different from zero and varied from molecule to molecule (see e.g. monomer in Figure 7b with $P \approx -0.75$). A similar behavior was displayed by individual *O* polyisocyanides, which could even show changes in *P* between different intensity levels of the same molecule, as observed in Figure 9b. In this case, a very minor variation in fluorescence lifetime (Figure 9c)[35] and a slight blue shift of the spectrum (Figure 9d)[35] are concurrent to the change in *P*, thus suggesting that one of the emitting units of the oligomer was affected by photobleaching.

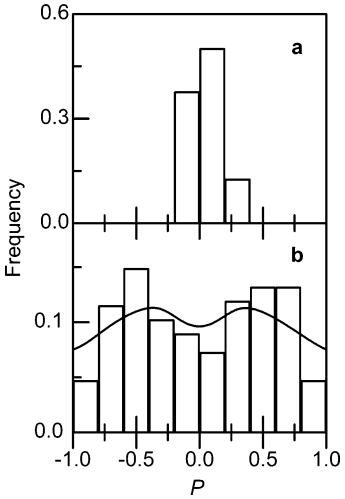

Figure 10. Distributions of polarization anisotropy for (a) 24 type *P* polymer molecules and (b) 215 monomer molecules. The solid line in b corresponds to the polarization anisotropy histogram simulated for a set of randomly oriented immobilized single emitting dipoles excited with circularly polarized light.[36,37]

In Figure 10a the polarization anisotropy distribution for a set of helical polymers is shown. As a reference, the same distribution is depicted for a collection of monomers in Figure 10b. The histogram obtained for individual PDI monomers reproduces the behavior expected for a set of randomly oriented single individual emitting dipoles which are excited with circularly polarized light.[36,37] Clearly, this typical single emitting dipole behavior is not observed for type *P* polyisocyanides, which show a very narrow *P* distribution around $P = 0$. One possible explanation for the lack of polarization in the emission of these polymers is the occurrence of a large number of emitting sites, each one having a different emitting dipole orientation. As a consequence, the polarization information stemming from each emitting site washes out, resulting in depolarization of the detected fluorescence. However, in our case it should be noted that the range of possible dipole orientations for emitters attached to the helical polyisocyanide backbone is limited due to geometrical restrictions. Arrangements of the transition dipole of the emitting excimer-like species parallel to the polymer axis are hardly probable, making a complete depolarization of the emission ($P \approx 0$) unlikely. On the other hand, as a result of the same geometrical restrictions, it can be expected that only a few emitting sites in the helical polyisocyanide are placed in an in-plane conformation with respect to the sample surface, and most of them will be in an out-of-plane conformation. Since out-of-plane dipole moments preferentially contribute to *P* values close to zero, the total fluorescence arising from a large amount of these sites is expected not to show a defined polarization direction, consistent with our experimental observations.

Figure 11 shows the distribution of the fluorescence intensities at $t = 0$ for type *P* helical polymers and, as a reference, also for the PDI monomers. The histogram of the monomers is rather narrow, while the distribution found for the type *P* polyisocyanides is much wider, as expected given the high polymer polydispersity (cf. Figure 2). Surprisingly, the polymeric PDI arrays, which contain hundreds to thousands of chromophore units, possess an average $I(t = 0)$ value (1.2×10^6 photons/s) that is only ca. 3 times larger than that of the monomer (0.43×10^6 photons/s). The lower fluorescence quantum yield measured in bulk for the excimer-like species in the PDI polyisocyanides ($\Phi_{polymer}/\Phi_{monomer} = 0.11$) cannot solely account for this result.

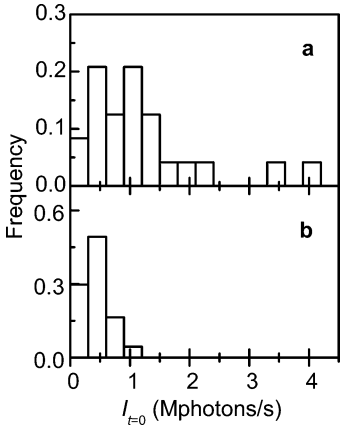

Figure 11. Distributions of fluorescence intensity at $t = 0$ for (a) 24 type *P* polymer molecules and (b) 67 monomer molecules.

To understand the low fluorescence intensity emission of the type *P* polymers, we made use of the single molecule fluorescence lifetime measurements. Two main features are evident from these experiments (see Figure 8c). First, the fluorescence decays obtained for the individual helical PDI polyisocyanides cannot be fitted by a simple monoexponential function even for very short bin times (see Figure S2 in the Supporting Information). Instead, multiexponential and stretched exponential models describe much better the experimental results. This is a clear indication that a heterogeneous population of emitting sites with distinct fluorescence lifetimes coexist in long helical PDI polyisocyanides. Second, a decrease of τ in time (very fast at short *t*, smoother later on) is observed in all type *P* polymer fluorescence lifetime trajectories, as illustrated in Figure 8c. Since the emission spectrum remains constant (see Figure 8d), the decrease of τ upon chromophore photobleaching must be ascribed to the formation of fluorescence traps, which partially quench the emission of the remaining fluorophore units.[38] Therefore, photodegradation of the emitting sites in helical perylenediimide pendant polyisocyanides must result in fluorescence quenching trap generation. The more traps are generated, the more accentuated must be the decrease in fluorescence lifetime, as observed in Figure 8c. Moreover, different distances between the emitting sites and the photogenerated quenching traps in the polymer will result in distinct effective fluorescence lifetimes, thus explaining the multiexponential nature of the fluorescence decays of individual polymer **8** molecules.

Interestingly, large characteristic lifetime values are encountered (above 10 ns in Figure 8c) at the very beginning of the fluorescence lifetime traces of the polymer. These values are much larger than typical monomer fluorescence lifetimes ($\langle\tau\rangle = 3.5$ ns for 67 monomers) and resemble the results obtained in bulk for the excimer-like component of polymer **8** fluorescence ($\tau = 19.9$ ns). Together with spectral data, this result clearly demonstrates that the fluorescence of the helical PDI polyisocyanide stems from excimer-like emitting sites. However, even at $t = 0$ the fluorescence decays measured for single polymers are multiexponential and the characteristic lifetime values recovered are consistently shorter than those measured in bulk for excimer-like emitting species. We ascribe this phenomenon to the occurrence of photobleaching and trap formation during the imaging step preceding the fluorescence lifetime trajectory collection. Although the polymer molecules are illuminated for only a very short period of time when scanning ($\approx$50 ms), yet a significant decrease in fluorescence intensity and lifetime is expected as extrapolated from the rapid decay observed in Figure 8c for the initial time values (*I* and τ decrease 35 and 40%, respectively, after the first 100 ms for this particular trace). This would account for the shorter τ values found for the excimer-like species in the single-molecule experiments and also for the low fluorescence intensities collected for the long helical polymers compared to the monomers. Consistent with this reasoning, the free diffusion of molecules in solution and the much lower excitation power densities used in the ensemble measurements (more than 6 decades lower) must prevent photodegradation and trap formation, explaining the larger τ values obtained in bulk. Indeed, fluorescence lifetime measurements of PMMA films doped with very high concentrations of perylenediimide polyisocyanides show that the higher the excitation power, the more pronounced the decrease of τ, i.e. the more efficient the quenching trap formation process.

We cannot currently assign the nature of the quenching sites created in single type *P* perylenediimide polymers upon continuous irradiation. A plausible candidate for the photoderived fluorescence trap is a radical ion, a species known to be an efficient quencher of emission in conjugated molecules.[39] Indeed, fluorescence quenching due to radical trap formation is usually thought to be responsible for the reversible dark periods in the emission of individual single- and multiple-fluorophore systems, such as perylenediimide or peryleneimide monomers and aggregates.[31,40] In our case, the emission spectrum of the excimer-type species in polymer **8** largely overlaps the absorption spectra reported for perylenediimide radical anions,[41] which ranges from 600 to 750 nm. Therefore, a very efficient energy transfer from the excimer-type species to nearby photogenerated PDI radical anions is expected, resulting in the quenching of the emission from the polymer.

PDI radical ions could originate from photoinduced intermolecular electron transfer between the polymer and an impurity in the sample (e.g. O_2, H_2O, the surrounding polymer matrix), a process in which either the photogenerated exciton or the subsequent excimer-like species formed in the helical PDI polymers could be involved. Such a phenomenon has been recently demonstrated to occur in individual peryelendiimide monomers and aggregates.[40d] In those cases, however, electron transfer to impurities and radical formation are rare events only occurring after millions of emitted photons, whereas in our study quenching trap generation appears to be a very efficient process. Moreover, preliminary measurements on PDI polyisocyanides/PMMA samples immersed in a N_2 atmosphere still showed a rapid decay of fluorescence intensity and lifetime for individual type *P* molecules, ruling out a major contribution of O_2 to quenching trap formation. On the other hand, efficient quenching trap generation was also observed for PDI polyisocyanides directly adsorbed on glass, which suggests a minor effect of the surrounding PMMA layer in the present measurements.

An alternative explanation for charge separation and radical ion generation is the occurrence of an intramolecular electron-transfer process, i.e., within one polymer chain. Such a process was observed to take place in individual dendrimers containing a central peryleneimide molecule (acceptor) and several triphenilamine groups (donor) at the rim.[42] Even more interesting, electron transfer between well-separated (>1.3 nm) PDI units to yield a PDI radical anion/PDI radical cation complex was recently proposed as the origin for the reversible long dark states in individual PDI dimers.[31c,43] Since the electron-transfer rate decays exponentially with the distance, we expect a much higher tendency for charge separation between the closely packed PDI moieties in compound **8**, which would explain the extremely fast fluorescence trap formation found for these species upon

irradiation. Indeed, recent works on π-stacked arrays of perylenediimides have demonstrated very efficient fluorescence quenching due to intramolecular charge separation between two neighboring PDI molecules separated by less than 1 nm.[44] However, fast charge recombination of the resulting PDI radical cation and anion was also observed to occur in that case.[44] At this point it must be noted that to act as an effective quenching mechanism in PDI polyisocyanides, the intramolecular charge separation should be long-lived (for instance, by charge migration through the polymer) or be followed by capture of the cation by some impurity so that the remaining PDI anion species can act as quencher. Further studies to prove the occurrence of these processes and, therefore, intramolecular electron transfer in long helical perylenediimide polyisocyanides are in progress.

Conclusions

In this work we have reported on the synthesis and characterization of perylenediimide polyisocyanides. Together with short oligomers, our synthetic approach yields long, well-defined, and rigid perylenediimide polymers with a helical backbone. This is achieved by exploiting the occurrence of hydrogen bonding interactions between the side groups of amino acid derived polyisocyanides. The rodlike nature of the synthesized polymers and the helical arrangement of the chromophores are demonstrated by means of atomic force microscopy, whereas bulk optical spectroscopy confirms the close-packing and chiral organization of the dyes. We have also presented a thorough single-molecule fluorescence investigation of the synthesized polymer fibers, which allows us to distinguish between short oligomers with an ill-defined chromophore arrangement and the relevant long helical perylenediimide polyisocyanides. The emission of these large chromophore assemblies is fully depolarized and characterized by a red-shifted spectrum accompanied by a long fluorescence lifetime consistent with the formation of multiple excimer-like species in the polymer. Upon continuous irradiation, fluorescence traps are efficiently generated. A plausible mechanism for this process would be perylenediimide radical anion formation by intramolecular electron transfer. This ability to yield charge separation upon excitation, in combination with exciton interactions between nearby chromophores and the occurrence of relatively long-lived emissive sites, would make the synthesized perylenediimide pendant polyisocyanides good candidates as n-type semiconductors for all organic solar cell construction.

Acknowledgment. This work was supported by the Dutch National Science Foundation. Financial support from the EC SMARTON network is also acknowledged. J.H. thanks the Spanish Ministry for Science and Technology for a Ramón y Cajal Fellowship. E.M.H.P.v.D. thanks the Dutch Foundation for Fundamental Research of Matter (FOM) for support.

Supporting Information Available: Details on the synthesis procedure and the materials used, the fractionation experiments, and the methods employed to characterize the perylenediimide polyisocyanides. This material is available free of charge via the Internet at http://pubs.acs.org.

References and Notes

(1) (a) Meyer, J.-P.; Schlettwein, D.; Wöhrle, D.; Jaeger, N. I. *Thin Solid Films* **1995**, *258*, 317−324. (b) Horowitz, G.; Kouki, F.; Spearman, P.; Fichou, D.; Nogues, C.; Pan, X.; Garnier, F. *Adv. Mater.* **1996**, *8*, 242−245. (c) Struijk, C. W.; Sieval, A. B.; Dakhorst, J. E. J.; van Dijk, M.; Kimkes, P.; Koehorst, R. B. M.; Donker, H.; Schaafsma, T. J.; Picken, S. J.; van de Craats, A. M.; Warman, J. M.; Zuilhof, H.; Sudhölter, E. J. R. *J. Am. Chem. Soc.* **2000**, *122*, 11057−11066. (d) Dimitrakopoulos, C. D.; Malenfant, P. R. L. *Adv. Mater.* **2002**, *14*, 99−117.

(2) (a) Wöhrle, D.; Meissner, D. *Adv. Mater.* **1991**, *3*, 129−138. (b) Toshimitsu, T.; Hirota, N.; Noma, N.; Shirota, Y. *Thin Solid Films* **1996**, *273*, 177−180. (c) Schmidt-Mende, L.; Fechtenkötter, A.; Müllen, K.; Moons, E.; Friend, R. H.; MacKenzie, J. D. *Science* **2001**, *293*, 1119−1122. (d) Breeze, A. J.; Salomon, A.; Ginley, D. S.; Gree, B. A.; Tillmann, H.; Hörhold, H.-H. *Appl. Phys. Lett.* **2002**, *81*, 3085−3087. (e) Peumans, P.; Uchida, S.; Forrest, S. R. *Nature* **2003**, *425*, 158−162.

(3) Sirringhaus, H.; Brown, P. J.; Friend, R. H.; Nielsen, M. M.; Bechgaard, K.; Langeveld-Voss, B. M. W.; Spiering, A. J. H.; Janssen, R. A. J.; Meijer, E. W.; Herwig, P.; de Leeuw, D. M. *Nature* **1999**, *401*, 685−688.

(4) (a) Gregg, B. A. *J. Phys. Chem.* **1996**, *100*, 852−859. (b) Gregg, B. A.; Sprague, J.; Peterson, M. W. *J. Phys. Chem. B* **1997**, *101*, 5362−5369. (c) Adams, D. M.; Kerimo, J.; Olson, E. J. C.; Zaban, A.; Gregg, B. A.; Barbara, P. F. *J. Am. Chem. Soc.* **1997**, *119*, 10608−10619.

(5) Kazmaier, P. M.; Hoffmann, R. *J. Am. Chem. Soc.* **1994**, *116*, 9684−9691.

(6) Würthner, F. *Chem. Commun.* **2004**, *14*, 1564−1579.

(7) (a) Würthner, F.; Thalacker, C.; Diele, S.; Tschierske, C. *Chem. Eur. J.* **2001**, *7*, 2245−2253. (b) Gade, L. H.; Galka, C. H.; Williams, R. M.; De Cola, L.; McPartlin, M.; Dong, B.; Chi, L. *Angew. Chem., Int. Ed.* **2003**, *42*, 2677−2681. (c) Ahrens, M. J.; Sinks, L. E.; Rybtchinski, B.; Liu, W. H.; Jones, B. A.; Giaimo, J. M.; Gusev, A. V.; Goshe, A. J.; Tiede, D. M.; Wasielewski, M. R. *J. Am. Chem. Soc.* **2004**, *126*, 8284−8294. (d) Würthner, F.; Chen, Z.; Hoeben, F. J. M.; Osswald, P.; You, C.-C.; Jonkheijm, P.; Herrikhuyzen, J.v.; Schenning, A. P. H. J.; van der Schoot, P. P. A. M.; Meijer, E. W.; Beckers, E. H. A.; Meskers, S. C. J.; Janssen, R. A. J. *J. Am. Chem. Soc.* **2004**, *126*, 10611−10618. (e) Yan, P.; Chowdhury, A.; Holman, M. W.; Adams, D. M. *J. Phys. Chem. B* **2005**, *109*, 724−730.

(8) (a) Sautter, A.; Thalacker, C.; Heise, B.; Würthner, F. *Proc. Natl. Acad. Sci. U.S.A.* **2002**, *99*, 4993−4996. (b) Thalacker, C.; Würthner, F. *Adv. Funct. Mater.* **2002**, *12*, 209−218.

(9) (a) Würthner, F.; Sautter, A.; Schmid, D.; Weber, P. J. A. *Chem. Eur. J.* **2001**, *7*, 894−902. (b) You, C.-C.; Würthner, F. *J. Am. Chem. Soc.* **2003**, *125*, 9716−9725. (c) Dobrawa, R. Lysetska, M.; Ballester, P.; Gru, M.; Würthner, F. *Macromolecules* **2005**, *38*, 1315−1325.

(10) Guan, Y.; Zakrevskyy, Y.; Stumpe, J.; Antonietti, M.; Faul, C. F. J. *Chem. Commun.* **2003**, *7*, 894−895.

(11) (a) Gensch, T.; Hofkens, J.; Heirmann, A.; Tsuda, K.; Verheijen, W.; Vosch, T.; Christ, T.; Basché, T.; Müllen, K.; De Schryver, F. C. *Angew. Chem., Int. Ed.* **1999**, *38*, 3752−3756. (b) Langhals, H.; Speckbacher, M. *Eur. J. Org. Chem.* **2001**, *13*, 2481−2485. (c) Weil, T.; Reuther, E.; Müllen, K. *Angew. Chem., Int. Ed.* **2002**, *41*, 1900−1904.

(12) (a) Dotcheva, D.; Klapper, M.; Müllen, K. *Macromol. Chem. Phys.* **1994**, *195*, 1905−1911. (b) Langhals, H.; Jona, W. *Angew. Chem., Int. Ed.* **1998**, *37*, 952−955. (c) Neuteboom, E. E.; Janssen, R. A. J.; Meijer, E. W.; *Synth. Met.* **2001**, *121*, 1283−1284.; (d) Wang, W.; Wan, W.; Zhou, H. H.; Niu, S. Q.; Li, A. D. Q. *J. Am. Chem. Soc.* **2003**, *125*, 5248−5249.

(13) (a) Cornelissen, J. J. L. M.; Donners, J. J. J. M.; de Gelder, R.; Graswinckel, W. S.; Metselaar, G. A.; Rowan, A. E.; Sommerdijk, N. A. J. M.; Nolte, R. J. M. *Science* **2001**, *293*, 676−680. (b) Samori, P.; Ecker, C.; Gossl, I.; de Witte, P. A. J.; Cornelissen, J. J. L. M.; Metselaar, G. A.; Otten, M. B. J.; Rowan, A. E.; Nolte, R. J. M.; Rabe, J. P. *Macromolecules* **2002**, *35*, 5290−5294.

(14) de Witte, P. A. J.; Castriciano, M.; Cornelissen, J. J. L. M.; Monsù-Scolaro, L.; Nolte, R. J. M.; Rowan, A. E. *Chem. Eur. J.* **2003**, *9*, 1775−1781.

(15) Hernando, J.; de Witte, P. A. J.; van Dijk, E. M. H. P.; Korterik, J.; Nolte, R. J. M.; Rowan, A. E.; García-Parajó, M. F.; van Hulst, N. F. *Angew. Chem., Intl. Ed.* **2004**, *43*, 4045−4049.

(16) Demmig, S.; Langhals, H. *Chem. Ber.* **1988**, *121*, 225−230.

(17) Kaiser, H.; Lindner, J.; Langhals, H. *Chem. Ber.* **1991**, *124*, 529−535.

(18) Maiti, A. K.; Aroca, R.; Nagao, Y. *J. Raman Spectrosc.* **1993**, *24*, 351.

(19) Cornelissen, J. J. L. M.; Graswinckel, W. S.; Adams, P. J. H. M.; Nachtegaal, G. H.; Kentgens, A. P. M.; Sommerdijk, N. A. J. M.; Nolte, R. J. M. *J. Polym. Sci., Part A: Polym. Chem.* **2001**, *39*, 4255−4264.

(20) To perform the molecular modeling calculation, a helical structure of the polymer backbone was assumed, as previously observed for other amino acid derived polyisocyanides.[13,14]

(21) Ebenstein, Y.; Nahum, E. *Nano Lett.* **2002**, *2*, 945−950.

(22) Neuteboom, E. E.; Meskers, S. C. J.; Meijer, E. W.; Janssen, R. A. J. *Macromol. Chem. Phys.* **2004**, *205*, 217−222.

(23) According to exciton theory,[25a] dipole−dipole interaction between the neighboring PDI moieties i and $i + 1$ or $i + 3$ is expected to be very minor not only because of the larger interchromophoric distance (∼2.5 nm between their center-of-masses) but also due to the nearly perpendicular

orientation of the main transition dipole moments of these chromophore pairs ($\beta = 96°$).

(24) To calculate the exciton interaction for the dimer formed by PDI units i and $i + 4$, we have applied the formulae given in ref 25a to the geometry of the polymer drawn in Figure 3c and the PDI monomer absorption spectrum in Figure 4a.

(25) (a) Kasha M.; Rawls, H. R.; Ashaf El-Bayoumi, M. *Pure Appl. Chem.* **1965**, *11*, 371. (b) Bednarz, M.; Knoester, J. *J. Phys. Chem. B* **2001**, *105*, 12913−12923. (c) Didraga, C.; Klugkist, J. A.; Knoester, J. *J. Phys. Chem. B* **2002**, *106*, 11474−11486.

(26) Cornelissen, J. J. L. M.; Graswinckel, W. S.; Rowan, A. E.; Sommerdijk, N. A. J. M.; Nolte, R. J. M. *J. Polym. Sci., Part A: Polym. Chem.* **2003**, *41*, 1725−1736.

(27) (a) Ford, W. E.; Kamat, P. V. *J. Phys. Chem.* **1987**, *91*, 6373−6380. (b) Bisht, P. B.; Fukuda, K.; Hirayama, S. *Chem. Phys. Lett.* **1996**, *258*, 71−79.

(28) Reynders, P.; Kuhnle, W.; Zachariasse, K. A. *J. Phys. Chem.* **1990**, *94*, 4073−4082.

(29) Studies in our group on amino acid derived polyisocyanides have proven that at least 10−15 repeat units are necessary for the hydrogen bonding interactions between polymer side chains to stabilize the backbone helical conformation.

(30) The nondiffraction limited spots in the fluorescence images of PDI polymers embedded in PMMA were found to be mainly round instead of elongated, with fwhm values lower than 450 nm in all cases. Several factors can account for the absence of larger elongated fluorescent spots expected for the very long, micrometer-sized polymers. On one hand, according to Figure 2, only a small fraction of the polymers are expected to be long enough to give rise to clear elongated spots in the fluorescence images. Furthermore, due to the limited persistence length of hydrogen-bonded polyisocyanides (ca. 70 nm), interaction of the long polymers with the surrounding PMMA matrix may lead to a low degree of elongation, thus resulting in roundlike features in the fluorescence images. Indeed, the degree of elongation of spin-coated PDI polyisocyanides has been found to depend on the environment: elongated polymer fibers were observed on bare mica and glass, while collapsed structures were found on graphite. However, it is important to note that, if existing, those collapsed polymer fibers in PMMA show the same optical properties as elongated chains on glass previously investigated at the single-molecule level.[15]

(31) (a) Hofkens, J.; Maus, M.; Gensch, T.; Vosch, T.; Cotlet, M.; Köhn, F.; Herrmann, A.; Müllen, K.; De Schryver, F. C. *J. Am. Chem. Soc.* **2000**, *122*, 9278−9288. (b) Christ, T.; Petzke, F.; Bordat, P.; Herrmann, A.; Reuther, E.; Müllen, K.; Basché, T. *J. Lumin.* **2002**, *98*, 23−33. (c) Liu, R.; Holman, M. W.; Zang, L.; Adams, D. M. *J. Phys. Chem. B* **2003**, *107*, 6522−6526.

(32) Vosch, T.; Cotlet, M.; Hofkens, J.; Van Der Biest, K.; Lor, M.; Weston, K.; Tinnefeld, P.; Sauer, M.; Latterini, L.; Müllen, K.; De Schryver, F. C. *J. Phys. Chem. A* **2003**, *107*, 6920−6931.

(33) Stracke, F.; Blum, C.; Becker, S.; Mullen, K.; Meixner A. *J. Chem. Phys.* **2004**, *300*, 153−164.

(34) Christ, T.; Kulzer, F.; Bordat, P.; Basché, T. *Angew. Chem., Int. Ed.* **2001**, *40*, 4192−4195.

(35) $\tau = 3.4$ ns and 3.3 ns for the highest and lowest intensity levels in Figure 8a. The maximum of their fluorescence spectra are at $\lambda = 521$ and 527 nm, respectively.

(36) The theoretical histogram of the polarization anisotropy values was calculated solving the equations given in ref 37 for a random distribution of emitters which are excited with circularly polarized light by means of a 1.3 NA oil-objective. It was assumed no displacement between the absorption and emission transition dipoles of the molecules, as well as a detection window ranging from I_{max} to $0.14I_{max}$, where I_{max} and $0.14I_{max}$ correspond the highest and lowest fluorescence intensities of the PDI monomer molecules detected in this work.

(37) Ha, T.; Laurence, T. A.; Chemla, D. S.; Weiss, S. *J. Phys. Chem. B* **1999**, *103*, 6839−6850.

(38) (a) Ying, L.; Xie, X. S. *J. Phys. Chem. B* **1998**, *102*, 10399−10409. (b) Hernando, J.; van der Schaaf, M.; van Dijk, E. M. H. P.; Sauer, M.; García-Parajó, M. F.; van Hulst, N. F. *J. Phys. Chem. A* **2003**, *107*, 43−52.

(39) Seth, J.; Palaniappan, V.; Johnson, T. E.; Prathapan, S.; Lindsey, J. S.; Bocian D. F. *J. Am. Chem. Soc.* **1994**, *116*, 10578−10592.

(40) (a) Holman, M. W.; Liu, R. C.; Adams, D. M. *J. Am. Chem. Soc.* **2003**, *125*, 12649−12654. (b) Zondervan, R.; Kulzer, F.; Orlinskii, S. B.; Orrit, M. *J. Phys. Chem. A* **2003**, *107*, 6770−6776. (c) Haase, M.; Hubner, C. G.; Reuther, E.; Herrmann, A.; Müllen, K.; Basché, T. *J. Phys. Chem. B* **2004**, *108*, 10445−10450. (d) Hoogenboom, J. P.; van Dijk, E. M. H. P.; Hernando, J.; van Hulst, N. F.; García-Parajó, M. F. *Phys. Rev. Lett.* **2005**, *95*, 097401.

(41) Kircher, T.; Löhmannsröben, H. G. *Phys. Chem. Chem. Phys.* **1999**, *1*, 3987−3992.

(42) Gronheid, R.; Stefan, A.; Cotlet, M.; Hofkens, J.; Qu, J. Q.; Müllen, K.; Van der Auweraer, M.; Verhoeven, J. W.; De Schryver, F. C. *Angew. Chem., Int. Ed.* **2003**, *42*, 4209−4214.

(43) Holman, M. W.; Liu, R. C.; Zang, L.; Yan, P.; DiBenedetto, S. A.; Bowers, R. D.; Adams, D. M. *J. Am. Chem. Soc.* **2004**, *126*, 16126−16133.

(44) (a) Rybtchinski, B.; Sinks, L. E.; Wasielewski, M. R. *J. Am. Chem. Soc.* **2004**, *126*, 12268−12269. (b) Fuller, M. J.; Sinks, L. E.; Rybtchinski, B.; Giaimo, J. M.; Li, X.; Wasielewski, M. R. *J. Phys. Chem. A* **2005**, *109*, 970−975.